

Jahn-Teller instability in $C_6H_6^+$ and $C_6H_6^-$ revisited.

Vasili Perebeinos¹, Philip B. Allen², and Mark Pederson³

¹*Department of Physics, Brookhaven National Laboratory, Upton, New York 1973-5000,*

²*Department of Physics, Department of Physics and Astronomy,
State University of New York, Stony Brook, NY 11794-3800*

³*Naval Research Laboratory, Complex Systems Theory Branch, Washington, DC 20375-5345*

(Dated: October 24, 2018)

The benzene cation ($C_6H_6^+$) has a doublet (e_{1g}) ground state in hexagonal ring (D_{6h}) geometry. Therefore a Jahn-Teller (JT) distortion will lower the energy. The present theoretical study yields a model Hückel-type Hamiltonian that includes the JT coupling of the e_{1g} electronic ground state with the *two* e_{2g} vibrational modes: in-plane ring-bending and C-C bond-stretching. We obtain the JT couplings from density functional theory (DFT), which gives a JT energy lowering of 970 cm^{-1} in agreement with previous quantum chemistry calculations. We find a non-adiabatic solution for vibrational spectra and predict frequencies shifts of both the benzene cation and anion, and give a reinterpretation of the available experimental data.

PACS numbers: 31.50.Gh; 31.15.Ew; 31.30.Gs

I. INTRODUCTION

A molecular system with a degenerate electronic ground state will spontaneously lower its symmetry to lift the degeneracy. This is the Jahn-Teller (JT) [1] effect, and is common in molecules [2]. The C_6H_6 (benzene) molecule has a long history of study [3, 4]. The benzene cation represents a paradigm of the dynamical JT effect [5]. With full D_{6h} symmetry, the highest occupied molecular orbital (HOMO) e_{1g} is doubly degenerate, as is the lowest unoccupied molecular orbital (LUMO) e_{2u} . Hence both the cation and anion are JT unstable and prefer lower symmetry. In the lowest (linear) approximation, the Born-Oppenheimer surface has a degenerate loop in configuration space surrounding the D_{6h} ground state. Everywhere on this loop, the HOMO and LUMO states are split by a constant JT gap. The most symmetric points on this loop represent simple D_{2h} distortions. These distortions occur in three equivalent “acute” and three equivalent “obtuse” forms (see the inset to Fig. 2). Higher order corrections lift the degeneracy on the loop, but zero-point energy exceeds the barrier height, creating a dynamic rather than a static JT distortion.

Ab initio approaches [6, 7, 8] including density functional theory (DFT) [9, 10] have been used to predict the ground state geometry and the JT energy lowering in the benzene cation. Quantum chemistry methods have been used to analyze vibrational spectra of the benzene cation [11, 12, 13]. A high resolution zero-kinetic-energy (ZEKE) photoelectron study by Linder *et al.* [14] found values of the frequency shift of the in-plane ring-bending e_{2g} vibrational mode. From their analysis, they deduced the JT energy lowering to be 208 cm^{-1} . They also concluded that the cation has a global minimum for the acute D_{2h} geometry, with a local minimum for the obtuse geometry only 8 cm^{-1} higher in energy. *Ab initio* calculations [8] suggest 4-5 times greater energy gain. The present study reconciles this discrepancy. We provide a microscopic model Hamiltonian for the π -electron sys-

tem, which includes two independent e_{2g} modes of JT coupling. We derive all parameters of this model from DFT calculations and find vibrational spectra for both the cation and anion using a non-adiabatic approximation. Our results for the cation permit a reinterpretation of the ZEKE spectra, allowing a larger JT energy lowering, which agrees with both our DFT and previous theory.

II. MODEL HAMILTONIAN

The starting point is a Hückel-type Hamiltonian for the non-bonding π electrons, with a first-neighbor hopping integral $t_1 = -\langle i|\mathcal{H}|i\pm 1\rangle$ between adjacent p_z atomic orbitals on the six C atoms. In Slater-Koster notation [15], $-t_1$ is called the $(pp\pi)$ two-site integral. In the D_{6h} point group, all six t_1 integrals are the same. The 6-dimensional electronic Hilbert space has single-particle states with a_{2u} , e_{1g} , e_{2u} , b_{1g} symmetries, which have energies $-2t_1, -t_1, t_1, 2t_1$.

Hopping matrix elements t decrease with distance between atoms. For small atomic displacements, t depends linearly on the C-C bond length, $t_1(\delta R_{i,i+1}) = t_1^0 - g_1\delta R_{i,i+1}$. The electron-phonon coupling constant g_1 is the same as in the Su-Schrieffer-Heeger model[16] for polyacetylene. Next we introduce second neighbor hopping $t_2 = \langle i-1|\mathcal{H}|i+1\rangle = t_2^0 + g_2\delta\alpha_i$ to include a dependence on the change $\delta\alpha_i$ of the C_{i-1} - C_i - C_{i+1} bond angle α_i from 120° . The constant term t_2^0 does not lift the degeneracy of the e levels. Therefore we put $t_2^0 = 0$ to keep the Hamiltonian as simple as possible. We use harmonic restoring forces K_1, K_2 for the bond stretching and angle bending vibrations. The total Hamiltonian

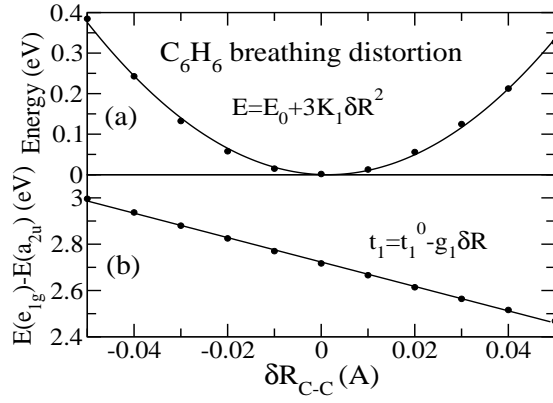


FIG. 1: (a) DFT total energy for neutral benzene with a symmetric a_{1g} distortion around the equilibrium C-C separation (closed circles). (b) Eigenvalue difference for the two lowest π states (closed circles). The C-H bond lengths are held fixed for both calculations. The solid curves are best fits using the model Hamiltonian Eq. (1) with g_1 and K_1 adjusted.

$\mathcal{H} = \mathcal{H}_{\text{el}} + \mathcal{H}_{\text{vib}}$ has the form

$$\begin{aligned} \mathcal{H}_{\text{el}} &= \sum_{i=1}^6 [-t_1^0 + g_1\delta R_{i,i+1}|i\rangle\langle i+1| \\ &\quad + g_2\delta\alpha_i|i-1\rangle\langle i+1| + h.c.] \\ \mathcal{H}_{\text{vib}} &= \sum_{i=1}^6 (P_i^2/2M + K_1\delta R_{i,i+1}^2/2 + K_2\delta\alpha_i^2/2). \end{aligned} \quad (1)$$

The coupling constants $g_{1,2}$ and spring constants $K_{1,2}$ are calculated from DFT using the program NRLMOL[17] with a Gaussian basis set and the Perdew-Burke-Ernzerhof exchange-correlation potential [18]. This yields as the optimal geometry of neutral benzene in D_{6h} symmetry, the C-C and C-H bond lengths of $R_0 = 1.398$ Å and 1.08 Å respectively. The energy difference between the HOMO e_{1g} and a_{2u} orbitals defines the hopping integral $t_1^0 = 2.72$ eV. We fix the C-H bond length and introduce a symmetric a_{1g} breathing distortion, which alters the C-C bond lengths. The results, shown on Fig. (1), can be fitted to the predictions of the model Hamiltonian (1) $E = E_0 + 3K_1\delta R^2$ (for the total energy) and $\Delta E = t_1 = t_1^0 - g_1\delta R$ for the $E(e_{1g}) - E(a_{2u})$ eigenvalue difference. The results are $g_1 = 5.27$ eV/Å and $K_1 = 47.4$ eV/Å².

Second neighbor integrals are found from DFT energies for distortions with D_{2h} symmetry. We fixed the C-C bond lengths and varied the bond angle $\delta\alpha$ as shown in the inset to Fig. (2). Specifically, angles 1 and 4 were decreased by 2α , while the remaining four angles were increased by α . The hydrogen atoms were fixed along the bisectors of the C-C-C angles. The results were fitted to the predictions of the Hamiltonian (1) $E = E_0 + 6K_2\delta\alpha^2$ for the total energy, and $4g_2\delta\alpha$ for the splitting of doubly degenerate e_{1g} HOMO states into b_{2g} and b_{3g} singlets. The results are $K_2 = 7.45$ eV/rad² and $g_2 = 0.91$ eV/rad.

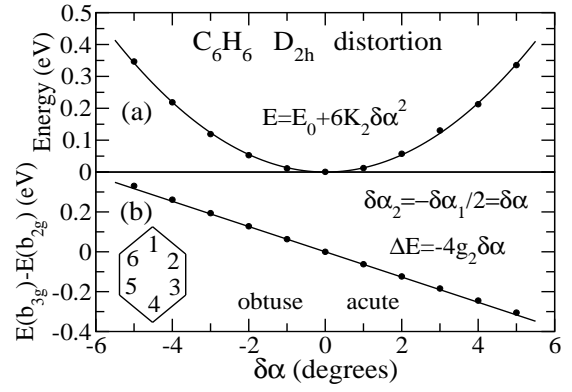


FIG. 2: (a) DFT total energies and (b) splitting of the doublet HOMO eigenvalues of neutral benzene with a D_{2h} distortion and fixed C-C bond lengths as shown in the inset. The solid curves are best fits using the model Hamiltonian Eq. (1) to fix the parameters g_2 and K_2 .

	Model		DFT	
δR_0 (Å)	0.018	(0.018)	0.014	(0.022)
δE_1 (eV)	-0.049	(-0.049)	-0.028	(-0.046)
	acute	obtuse	acute	obtuse
$\delta\alpha_1 = -2\delta\alpha$	2.36°	-2.38°	1.65°	-1.73°
δE_2 (eV)	-0.019	-0.019		
$\delta R'_1$ (Å)	0.020	-0.020	0.020	-0.020
$\delta R'_2$ (Å)	-0.040	0.040	-0.037	0.042
δE_3 (eV)	-0.105	-0.108		
$\Delta E_{\text{JT}}^{\text{tot}}$ (eV)	-0.124	-0.127	-0.123	-0.120
$2\Delta_{\text{JT}}$ (eV)	0.497	0.508	0.500	0.481

TABLE I: The geometry and energies of the model Hamiltonian and DFT solutions for the benzene cation. The breathing a_{1g} mode relaxation for the anion are shown in brackets.

III. ADIABATIC SOLUTION

For fixed atomic coordinates, the adiabatic potential energy surface (APES) can easily be calculated using Eq. (1). For the D_{2h} distortion shown in the inset of Fig. (2), the energy depends on three variables $\delta R_1 = \delta R_{12}$, $\delta R_2 = \delta R_{23}$ and $\delta\alpha_2 = -\delta\alpha_1/2 = \delta\alpha$. The electronic contribution is the sum of the occupied eigenvalues of Eq. (1). The energy is not analytic at the point $(\delta R_1, \delta R_2, \delta\alpha) = (0, 0, 0)$, but has a cusp, characteristic of the first-order JT splitting. Charged benzene lowers its energy by $\delta E_1 + \delta E_2 + \delta E_3$ corresponding to atomic relaxation *via* three types of vibrational modes. The first is the symmetric A_{1g} distortion of D_{6h} symmetry, $\delta R_1 = \delta R_2 = \delta R_0$ and $\delta\alpha = 0$. The second and the third are two E_{2g} vibrational modes: the ring-bending and C-C bond-length distortions. It is more convenient to measure distortions $\delta R'$ around the relaxed breathing positions $R = R_0 + \delta R_0 = 1.416$ Å. The distorted geometry of benzene ions and corresponding energy gains are shown in Table I.

The geometry and energies of the DFT solution (Table

I) are reasonably well reproduced by the model Hamiltonian. The energy difference (3.7 meV) found between the acute or obtuse distortions is sensitive to the choice of exchange-correlation potential and smaller than the errors of calculations [9]. The DFT energy lowering and carbon atomic distortions are affected by hydrogen distortions as well, which are left out completely in Eq. (1). We did constrained geometry optimization with hydrogens forced to follow carbons so that C-H bond divides C-C-C angle by half. The minimum energy in the constrained calculations was only 4 meV higher in energy than in the fully optimized geometry for both acute and obtuse cations. The main conclusion is that the C-C bond-length distortions contribute the most to the JT energy lowering and degenerate level splitting in both the benzene cation and anion.

IV. VIBRATIONAL MODEL HAMILTONIAN

JT-coupled vibrational modes change their frequencies on a charged molecule. The observable frequency shifts serve as a measure of the JT energy lowering. We solve the model Hamiltonian for the vibrational spectra for both cation and anion. For the case of the cation, the Hamiltonian (1) is projected on the two e_{1g} HOMO states with symmetries b_{3g} and b_{2g} in the D_{2h} point group,

$$\begin{aligned} |b_{3g}\rangle &= \frac{1}{\sqrt{12}} (2|1\rangle + |2\rangle - |3\rangle - 2|4\rangle - |5\rangle + |6\rangle) \\ |b_{2g}\rangle &= \frac{1}{2} (|2\rangle + |3\rangle - |5\rangle - |6\rangle) \end{aligned} \quad (2)$$

The Hamiltonian takes form $U_1 H U_1^\dagger = H_0 \hat{I} + H_z \sigma_z + H_x \sigma_x$, where $U_1 = (|b_{3g}\rangle, |b_{2g}\rangle)$, and σ_β are the Pauli matrices in the $\{b_{3g}, b_{2g}\}$ subspace,

$$\begin{aligned} H_0 &= \sum_{i=1}^6 \left(P_i^2 / 2M + K_1 \delta R_{i,i+1}'^2 / 2 + K_2 \delta \alpha_i'^2 / 2 \right) \\ H_z &= \frac{g_1}{6} (\delta R_1' + \delta R_3' + \delta R_4' + \delta R_6' - 2\delta R_2' - 2\delta R_5') \\ &\quad + \frac{g_2}{2} (\delta \alpha_1 + \delta \alpha_4) \\ H_x &= \frac{g_1}{\sqrt{12}} (\delta R_1' - \delta R_3' + \delta R_4' - \delta R_6') \\ &\quad + \frac{g_2}{\sqrt{12}} (\delta \alpha_2 - \delta \alpha_3 + \delta \alpha_5 - \delta \alpha_6) \end{aligned} \quad (3)$$

In adiabatic approximation, the JT orbital splitting is $2\Delta = 2g_1^2/3K_1 + 2g_2^2/3K_2$ and the JT energy lowering is $E_{JT} = -\Delta/2$. To solve the problem beyond the adiabatic approximation we have to quantize vibrational motions. We rewrite the Hamiltonian (3) in Cartesian coordinates $(\delta x_i, \delta y_i)$. The kinetic energy term is diagonal. Choosing as the unit of displacement $R=1.416 \text{ \AA}$ (the benzene ring radius after a_{1g} mode relaxation), and as the energy unit $K_1 R^2$, the potential energy of the Hamiltonian H_0 (Eq. (3)) depends on a single parameter $K_2/K_1 R^2 = \Lambda$.

After diagonalizing H_0 we get twelve normal modes whose amplitudes we designate $\Theta_{1..12}$. The potential energy is independent of the motion of the center of mass ($X = \sum x_i, Y = \sum y_i$) and the ring rotation ($\alpha = \sum \alpha_i$). This forces three normal modes to have frequencies zero. Since we neglect C-H stretching motions, the mass M is $M_C + M_H$. Choosing $\Lambda = 0.0784$ the nine remaining normal modes are: the degenerate ring bending E_{2g} mode at $\omega_1 = 581 \text{ cm}^{-1}$ with some admixture of the C-C bond length alteration, the pure ring bending B_{1u} mode at 962 cm^{-1} , the breathing A_{1g} mode at 992 cm^{-1} , the mostly C-C bond-length-alteration doublets E_{1u} and E_{2g} at 1262 cm^{-1} and $\omega_2 = 1644 \text{ cm}^{-1}$ and the pure C-C bond-stretching mode B_{2u} at 1718 cm^{-1} . It is interesting to compare the model Hamiltonian normal mode spectrum with the DFT NRLMOL calculations. There are 21 in-plane vibrational modes $\Gamma = 2A_{1g} + A_{2g} + 4E_{2g} + 2B_{1u} + 2B_{2u} + 3E_{1u}$. Six of them are high frequency C-H modes $A_{1g} + B_{1u} + E_{1u} + E_{2g}$ around 3100 cm^{-1} . From the remaining 15 vibrations we identify the ring-bending E_{2g} mode at 600 cm^{-1} , the breathing A_{1g} at 992 cm^{-1} , and the bond-stretching E_{2g} at 1589 cm^{-1} .

The off diagonal part H_x of the Hamiltonian (3) depends only on the two JT-active E_{2g} vibrational normal modes. Let us label the amplitudes of these modes by $(\Theta_{1a}, \Theta_{1b})$ and $(\Theta_{2a}, \Theta_{2b})$ and denote their frequencies by ω_1 (ring bending) and ω_2 (bond-stretching) as above. We also use the coordinates Θ_1, Θ_2 to denote the total displacements $\Theta_1^2 = \Theta_{1a}^2 + \Theta_{1b}^2$ etc. Then Eq. (3) becomes:

$$\begin{aligned} H_0 &= \frac{M}{2} (\dot{\Theta}_{1a}^2 + \dot{\Theta}_{1b}^2 + \omega_1^2 \Theta_1^2) \\ &\quad + \frac{M}{2} (\dot{\Theta}_{2a}^2 + \dot{\Theta}_{2b}^2 + \omega_2^2 \Theta_2^2) \\ H_z &= -G_1 \Theta_1 \cos(\beta_1) - G_2 \Theta_2 \cos(\beta_2) \\ H_x &= -G_1 \Theta_1 \sin(\beta_1) - G_2 \Theta_2 \sin(\beta_2), \end{aligned} \quad (4)$$

where the angles β_1, β_2 contain arbitrary additive constants which are the choices of the orientation angles of the orthogonal eigenvectors in the two-dimensional E_g subspaces of the two modes. Note that the adiabatic electronic eigenvalues which diagonalize $H_z \sigma_z + H_x \sigma_x$ (in the approximation that $(\Theta_{1a}, \dots, \Theta_{2b})$ are classical variables) are $\pm \Delta_{JT}$ where

$$\Delta_{JT}^2 = G_1^2 \Theta_1^2 + G_2^2 \Theta_2^2 + 2G_1 G_2 \Theta_1 \Theta_2 \cos(\beta_1 - \beta_2) \quad (5)$$

This does not depend separately on the angles β_1, β_2 . The modified electron-phonon coupling constants G_1, G_2 depend on the JT couplings g_1, g_2 and on the E_g normal mode eigenstates. For our case ($\Lambda = 0.0784$) we find

$$\begin{aligned} G_1 &= T_1 g_1 / 6 + T_2 g_2 / 2R = 1.3 \text{ eV/\AA} \\ G_2 &= T_3 g_1 / 6 - T_4 g_2 / 2R = 4.14 \text{ eV/\AA} \end{aligned} \quad (6)$$

Let us consider further the adiabatic eigenstates of $\mathcal{H} = H_z \sigma_z + H_x \sigma_x$. What happens when we change

the angle $\delta\beta_1 = \delta \tan^{-1} \Theta_{1b}/\Theta_{1a}$? The rotation matrix $R = \cos(\alpha/2)\hat{\sigma}_z + i \sin(\alpha/2)\hat{\sigma}_x$ has the property that $R\mathcal{H}R^\dagger$ gives a new matrix \mathcal{H}' with angles $\beta_1 \rightarrow \beta_1 + \alpha$ and $\beta_2 \rightarrow \beta_2 + \alpha$. The energies $\pm\Delta_{JT}$ are unchanged and the eigenfunctions are rotated in (b_{3g}, b_{2g}) space by $\alpha/2$. This type of change of distortion pattern is called a “pseudo-rotation”. A full pseudo-rotation by $\alpha = 2\pi$ restores the molecular geometry and changes the sign of the electronic eigenstate. This sign change under adiabatic distortion is the Berry phase, and needs to be correctly incorporated when finding the system’s total wavefunction in adiabatic approximation. In particular it leads to fractional quanta of pseudorotational angular momentum. Our method will find total wavefunctions without making the adiabatic approximation and will therefore yield correct answers without explicit mention of Berry phase.

V. NON ADIABATIC SOLUTION

The quantized vibrational Hamiltonian (4) depends on three parameters $\omega_1/\omega_2 = 0.353$ and the two electron-phonon coupling constants $\kappa_1 = (\Delta_1/\hbar\omega_1)^{1/2} = 1.18$, $\kappa_2 = (\Delta_2/\hbar\omega_2)^{1/2} = 0.8$, where $\Delta_1 = G_1^2/M\omega_1^2 = 817\text{cm}^{-1}$ and $\Delta_2 = G_2^2/M\omega_2^2 = 1052\text{cm}^{-1}$ are twice the JT energy gain due to the ring-bending and the bond stretching modes correspondingly. Similar values of $\kappa_1 = 1.06$ and $\kappa_2 = 0.817$ were obtained by Eiding *et al.* [13] using *ab initio* many body techniques.

To solve Eq. (4) for the vibrational spectrum, assume for the moment a zero coupling to the bond stretching vibrational mode $G_2 = 0$. Then Eq. (4) depends on a single parameter κ_1 . The classical solution of Longuet-Higgins *et al.* [5] uses polar coordinates, which simplifies equations. Instead we seek the solution of Eq. (4) in the form

$$|\Psi\rangle = \sum_{n_1=0}^N \sum_{n_2=0}^{N-n_1} \left[A_{n_1, n_2} \frac{(c_a^\dagger)^{n_1}}{\sqrt{n_1!}} \frac{(c_b^\dagger)^{n_2}}{\sqrt{n_2!}} |0\rangle |b_{3g}\rangle + B_{n_1, n_2} \frac{(c_a^\dagger)^{n_1}}{\sqrt{n_1!}} \frac{(c_b^\dagger)^{n_2}}{\sqrt{n_2!}} |0\rangle |b_{2g}\rangle \right] \quad (7)$$

Note that we are not making the adiabatic approximation where the electronic wavefunction Ψ_{el} is strictly held in the lower of the two Jahn-Teller split levels. In adiabatic approximation the double valuedness of Ψ_{el} under rotation by $\beta = 2\pi$ is compensated by a restriction on the vibrational wavefunctions. This effect is automatically handled in our non-adiabatic treatment. The operators c_a^\dagger, c_b^\dagger create harmonic oscillator states in the two-dimensional manifold of e_g vibrations, with their origin at the symmetric (D_{6h}) benzene ion coordinates. Although different from the basis of Longuet-Higgins *et al.* [5], both basis sets are complete and converge rapidly to the same solution. The solution is found by exact diagonalization of Eq. (4) for $N = 10$. The eigenvalues

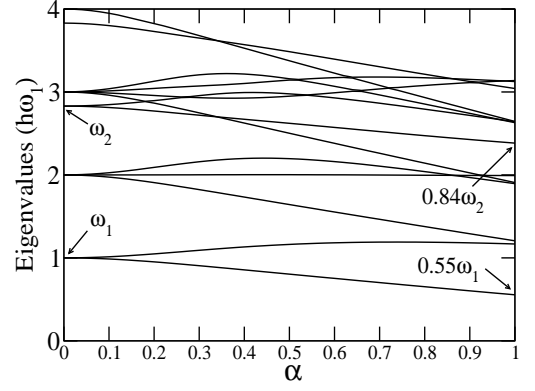


FIG. 3: Vibrational spectrum of the Jahn-Teller unstable ion *versus* parameter α , where coupling constants $\kappa_1 = 1.18 * \alpha$ and $\kappa_2 = 0.8 * \alpha$. For the cation, the coupling constant for the ring bending mode is $\kappa_1 = 1.18$ and coupling to the bond stretching mode is $\kappa_2 = 0.8$. Therefore for $\alpha = 1$ the neutral molecule vibrational frequency $\omega_1 = 581 \text{ cm}^{-1}$ becomes $0.55\omega_1$ and $\omega_2 = 1644 \text{ cm}^{-1}$ reduces to $0.84\omega_2$ for the cation.

coincides with those of Linder *et al.* [14] for the case of zero quadratic coupling.

The vibrational frequencies on the neutral molecule $\omega_1 = 581 \text{ cm}^{-1}$ and $\omega_2 = 1644 \text{ cm}^{-1}$ become (for the benzene cation) $0.54\omega_1$ and $0.7\omega_2$ in the uncoupled-mode approximation. To take into account the interaction between the two E_{2g} vibrational modes (when both $G_1 \neq 0$ and $G_2 \neq 0$) one has to use a trial wavefunction similar to Eq. (7), but including all four vibrational modes. The size of the matrix grows as $2 \times C_{N+4}^4 \approx (N + 2.5)^4/12$. Convergence was reached for $N = 10$. The lowest eigenvalues as a function of parameter α are shown on Fig. 3. The coupling constants are proportional to α and at $\alpha = 1$ they become $\kappa_1 = 1.18$ and $\kappa_2 = 0.8$. The frequency shift of the ring bending mode $\omega_1 \rightarrow 0.55\omega_1$ is essentially the same as in the noninteracting case. The interaction of the bond stretching mode with the ring bending overtones results in the level repulsion, such that $\omega_2 \rightarrow 0.84\omega_2$ for $\kappa_2 = 0.8$. The predicted vibrational spectrum corresponds to $\alpha = 1$ on Fig. 3.

On the anion, a D_{2h} distortion splits the e_{2u} LUMO into two b_{1u} and a_u orbitals, which can be obtained from Eq. (2) by changing the sign in front of the $|2\rangle, |4\rangle, |6\rangle$ molecular orbitals. Projecting the Hamiltonian Eq. (1) into the $\{b_{1u}, a_u\}$ manifold leads to the same Hamiltonian as (4) with a sign change of coupling constant $g_1 \rightarrow -g_1$. The vibrational excitation spectra on the anion $C_6H_6^-$ is described by Eq. (4), with coupling constants $G'_1 = -T_1g_1/6 + T_2g_2/2R_0 = 0.17 \text{ eV/\AA}$ and $G'_2 = -T_3g_1/6 - T_4g_2/2R_0 = -5.48 \text{ eV/\AA}$. Since the H_0 part of the projected Hamiltonian is the same as for the cation, the values for $T_{1..4}$ are unchanged. The JT energy lowering on the anion is the same as for the cation $G_1'^2/M\omega_1^2 + G_2'^2/M\omega_2^2 = 0.234 \text{ eV}$, but the effective couplings to the ring bending and C-C bond stretching modes are now different; $\kappa'_1 = 0.16$ and $\kappa'_2 = 1.06$ re-

spectively. This means that the frequency of the ring bending E_{2g} mode is shifted by less than 2% from the neutral benzene value, whereas the bond-stretching E_{2g} mode becomes 59% of the neutral molecule value 1644 cm^{-1} .

VI. SUMMARY

Using the model Hamiltonian Eq. (1) with DFT-calculated parameters, we predict the JT stabilization energy of 944 cm^{-1} for both the benzene cation and anion. The bond-stretching mode 1644 cm^{-1} on neutral benzene experiences a large shift on the anion and becomes 970 cm^{-1} , which is very close in energy to the a_{1g} breathing mode 992 cm^{-1} . On the other hand, the ring-bending mode is essentially unaffected. To the contrary, on the cation both E_{2g} JT active modes experience the sizable shifts by 45% and 16% from their neutral benzene values. Experimentally [14, 20] the ring-bending mode on the benzene cation was measured to reduce from 536 cm^{-1} to 350 cm^{-1} (or by 35%). This measurements led Linder *et al.* [14] to deduce a JT energy stabilization of 208 cm^{-1} . A more detailed analysis, including quadratic JT coupling, led to the conclusion that the acute D_{2h} distorted geometry is the global minimum, lower by 8 cm^{-1} than the obtuse local minimum. Our Hamiltonian (4) predicts a larger relative shift of the ring bending mode by 10% with respect to the experimental shift. The amount of the shift is sensitive to the choice of normal modes determined by the term \mathcal{H}_0 (Eq. 4), a slightly oversimplified model. The main result of our new solution is that there are **two** contributions to the JT energy lowering. To determine the JT energy lowering on the cation **two** vibrational E_{2g} frequencies have to be measured. The model Hamiltonian (1) contains quadratic couplings, which predict an acute global minimum, while the accuracy of the true DFT answer is insufficient to make such a prediction [9].

The benzene anion is not stable, which makes it difficult to measure the vibrational spectrum. Electron transmission techniques [21] give an opportunity to measure the vibrational sidebands in the resonant electron cross section at negative electron affinity 1.1 eV [21]. The spectrum shows vibrational peaks separated by 123 meV (or 992 cm^{-1}), and were attributed to a_{1g} vibrational quanta. The higher frequency JT-active e_{2g} mode has not been resolved. Our results, however, suggest that since both breathing and C-C bond stretching modes are coupled to the LUMO, a mixture of the two is expected to be present in the spectrum. Since the e_{2g} modes become very close in energy to the breathing a_{1g} mode, it is difficult to distinguish experimentally between the two.

In conclusion we derived a new model Hamiltonian for the JT active benzene cation and anion, and obtained all parameters from DFT calculations. This model Hamiltonian predicts a JT stabilization energy of 970 cm^{-1} . This value, similar to other first-principles results, is 4.5 times larger than the value deduced experimentally by Linder *et al.* [14]. However, our model gives the result that **two** E_{2g} modes are JT-active, coupling to the electronic HOMO and LUMO states. Only one of them was measured [14], and our results are reasonably consistent with that measurement. However, both modes are needed to obtain the JT stabilization energy from spectroscopic data. We conclude that there is no contradiction between theory and experiment, and predict the relevant frequency shifts that can be used to test theory more completely.

Acknowledgments

We are grateful to Prof. Philip M. Johnson for useful discussions. This work was supported in part by DOE Grant No. DE-AC-02-98CH10886, and in part by NSF Grant No. DMR-0089492.

-
- [1] H. Jahn and E. Teller, Phys. Rev. **49**, 874 (1936).
 - [2] I. B. Bersuker, Chem. Rev. **101**, 1067 (2001); T. A. Barckholtz and T. A. Miller, Int'l Rev. Phys. Chem. **17**, 435 (1998).
 - [3] G. B. Kistiakowsky and A. K. Soloman, J. Chem. Phys. **5**, 609 (1937).
 - [4] H. Sponer, G. Nordheim, A. L. Sklar, and E. Teller, J. Chem. Phys. **7**, 207 (1939).
 - [5] H. C. Longuet-Higgins, U. Öpik, M. H. L. Pryce, R. A. Sack, Proc. R. Soc. London, Ser. A **244**, 1 (1958).
 - [6] M. Engström, O. Vahtras, and H. Agren, Chem. Phys. **243**, 263 (1999).
 - [7] H. Köppel, L. S. Cederbaum, and W. Domcke, J. Chem. Phys. **89**, 2023 (1988).
 - [8] K. Raghavachari, R. C. Haddon, T. A. Miller, and V. E. Bondybey, J. Chem. Phys. **79**, 1387 (1983).
 - [9] K. Muller-Dethlefs and J. B. Peel, J. Chem. Phys. **111**, 10550 (1999).
 - [10] K. Yoshizawa, T. Kato, and T. Yamabe, J. Chem. Phys. **108**, 7637 (1998).
 - [11] N. O. Lipari, C. B. Duke, and L. Pietronero, J. Chem. Phys. **65**, 1165 (1975).
 - [12] P. Pulay, G. Fogarasi, and J. E. Boggs, J. Chem. Phys. **74**, 3999 (1981).
 - [13] J. Eiding, R. Schneider, W. Domcke, H. Köppel, and W. von Niessen, Chem. Phys. Lett. **177**, 345 (1991).
 - [14] R. Linder, K. Müller-Dethlefs, E. Wedum, K. Haber, E. R. Grant, Science **271**, 1698 (1996).
 - [15] J. C. Slater and G. D. Koster, Phys. Rev. **94**, 1498 (1954).
 - [16] W. P. Su, J. R. Schrieffer, and A. J. Heeger, Phys. Rev. Lett. **42**, 1698 (1979); Phys. Rev. B **22**, 2099 (1980).

- [17] M. R. Pederson and K. A. Jackson, Phys. Rev. B. **41**, 7453 (1990); K. A. Jackson and M. R. Pederson, Phys. Rev. B. **42**, 3276 (1990); M. R. Pederson and K. A. Jackson, Phys. Rev. B. **43**, 7312 (1991); D. V. Porezag and M. R. Pederson, Phys. Rev. B. **54**, 7830 (1996); A. Briley, M. R. Pederson, K. A. Jackson, D. C. Patton, and D. V. Porezag, Phys. Rev. B. **58**, 1786 (1998).
- [18] J. P. Perdew, K. Burke, and M. Ernzerhof, Phys. Rev. Lett. **77**, 3865 (1996).
- [19] M. V. Berry, Proc. R. Soc. London Ser. A **392**, 45 (1984).
- [20] J. G. Goode, J. D. Hofstein, and P. M. Johnson, J. Chem. Phys. **107**, 1703 (1997).
- [21] P. D. Burrow, J. A. Michejda, K. D. Jordan, J. Chem. Phys. **86**, 9 (1987).